

REC-2.00  
MY... 50.



1 SHOCKED GAS TEMPERATURE MEASUREMENTS BY INFRARED MONOCHROMATIC RADIATION "

2 PYROMETRY

3 by M. R. Lauver, J. H. Hall, and F. E. Belles

4 ABSTRACT

FACILITY FORM 802

N66-18342	(THRU)
(ACCESSION NUMBER)	
30	(CODE)
(PAGES)	
TMX 56330	33
(NASA CR OR TMX OR AD NUMBER)	(CATEGORY)

18342

5 The temperature history of a carbon dioxide-argon mixture was followed  
6 by an infrared monochromatic radiation pyrometer technique after incident  
7 and reflected shocks. Temperatures as high as 3600° K were measured.

8 One-dimensional wave theory calculations of the incident and reflected  
9 temperatures were found to be in good agreement with the experimental  
10 results. Detailed time-temperature studies showed the effect of attenuation  
11 and dissociation.

Author

AVAILABLE TO NASA OFFICES, NASA RESEARCH CENTERS  
[REDACTED]

12 INTRODUCTION

13 The shock tube has found one of its prime applications in the study  
14 of high-temperature rate processes in gases. Commonly, these processes  
15 have a strong temperature dependence, and it is therefore necessary to  
16 know the temperature of the experiment quite accurately. This need can be  
17 met nicely so long as incident shock waves are used to heat the gas,



E-3002

1 because one-dimensional theory, plus the thermodynamic properties of the  
2 gas, can be used to calculate the shocked-gas temperature from the measured  
3 velocity of the wave. Very often, however, it is convenient or even  
4 necessary to study processes behind reflected shocks, taking advantage of  
5 the higher temperatures and pressures which can be produced without unduly  
6 straining the capacities of conventional shock tubes. In that event, it  
7 is no longer so clear that the temperature can be calculated accurately;  
8 interactions of the reflected shock with the boundary layer (ref. 1) and  
9 with the pressure gradient created by attenuation of the incident shock  
10 (ref. 2) introduce ambiguities.

11 This problem has been widely recognized, and measurements of reflected-gas  
12 temperature have recently begun to appear in the literature. For the most  
13 part they were made by the line-reversal method (ref. 3,4),  
14 although in one case the rate of a chemical reaction was used as an  
15 indication of temperature (ref. 5). The purpose of the present work was  
16 to apply still another technique. We have determined the temperature  
17 from simultaneous measurements of infrared spectral emission and emissivity.

Among the advantages of the infrared method are the following: (1) There is no need to introduce sodium salts or other sources of emission; (2) good time resolution is possible; and (3) a very wide temperature range can be covered, not limited by the available brightness temperature of a light source, as in the reversal method.

This paper reports temperatures measured behind reflected shocks in a gas that is typical of mixtures likely to be used in chemical studies: 10% CO<sub>2</sub>-90% Ar. The temperature range behind reflected shocks was 2000° to 3600° K, although temperatures as low as 1000° K were measured behind incident waves. Temperatures determined at short times (50 to 100  $\mu$  sec) after the reflected wave passed the observation station are compared with values calculated from the velocity of the incident wave. Two detailed temperature-time records are also presented; these show the effects of shock attenuation on both the incident- and the reflected-shock temperature.

#### APPARATUS AND EXPERIMENTAL PROCEDURE

##### Basis of Emission-Absorption Pyrometry

The infrared monochromatic radiation (IMRA) method of gas temperature

1 measurement has been described elsewhere (ref. 6, 7). It is based on  
2 the fact that the intensity of radiation emitted by a hot gas depends on  
3 the gas temperature and on the number of gaseous entities (molecules, free  
4 radicals, or atoms) emitting radiation. Consequently, by measuring the  
5 absolute intensity of radiation (spectral emission) and the relative  
6 number density of emitters (spectral emissivity), the temperature of a  
7 gas can be calculated. Figure 1 shows schematically the information  
8 recorded in a shock-tube experiment, and the way in which it is reduced  
9 to a temperature measurement.

10 The measurement of spectral emission is straightforward. The infrared  
11 detection system response to the hot gas emission ( $V_g$ , fig. 1) is compared  
12 with its response to a calibrated standard infrared source ( $V_s$ ), and  
13 converted to absolute units by means of calibration factors. The result  
14 is a spectral emission value ( $I_g$ ) in terms of watts  $\text{cm}^{-2} \mu^{-1} \text{ster}^{-1}$  at  
15 a specific wavelength. The effect of the number of emitters is accounted  
16 for by absorption spectroscopy at the same wavelength. The reduction in  
17 signal strength due to transmitted light, from  $V_0$  to  $V$  volts, determines

the spectral absorptivity ( $1 - \frac{V}{V_0}$ ), which is equal to the spectral emissivity,  $e$ .

According to Kirchoff's radiation law, the ratio of the spectral emission of the hot gas to its spectral emissivity is numerically equal to the radiation ( $I_b$ ) that would be emitted by an ideal blackbody radiator at the same temperature as the gas:

$$\frac{I_g}{e} = I_b \quad (1)$$

Planck's law relating temperature to blackbody spectral emission is

$$I_b = C_1 \lambda^{-5} / (e^{C_2 / \lambda T} - 1) \quad (2)$$

Thus, inasmuch as  $C_1$  and  $C_2$  are physical constants and  $I_b$  is measured at the wavelength  $\lambda$ , the temperature is determined.

#### Apparatus for Emission-Absorption Pyrometry

A schematic diagram of the shock tube and associated equipment is given in figure 2. A constant intensity of infrared radiation from a glower source is mechanically chopped at 80 kilocycles per second and sent through the sapphire windows of the shock tube into a prism monochromator and a liquid-nitrogen-cooled indium antimonide detector. The shocked gases emit radiation which passes out of the shock tube into the same radiation

detection system. Its output is amplified by a directly-coupled circuit providing a measure of the gaseous emission intensity (the glower intensity is negligible in comparison to that of emission). The glower signal intensity is determined with a capacitor-coupled, tuned circuit of high gain. With these amplifiers, the detection system distinguishes between the emitted and transmitted light, although both are presented simultaneously to the one detector, and sends the resulting signals to different oscilloscope beams for recording.

#### Calibration of Pyrometer:

The IMRA apparatus was calibrated by ~~x~~ determining the transmittance of the shock tube window and the absolute radiance of the internal secondary-standard source (B in *Fig. 2*), which was a tungsten-ribbon lamp.

The window was found to pass 82 percent of  $4.5\mu$  radiation falling on it. This was the wavelength used for the temperature measurements.

Although the center of the asymmetric<sup>m</sup> stretching band of carbon dioxide is at  $4.3\mu$ , the longer wavelength is much more desirable. At  $4.5\mu$ ,

only the hot gas in the shock tube is optically active, while the cool carbon dioxide in the room and in the shock-tube boundary layer is almost completely transparent.

The internal standard was compared with a source which had been calibrated at the Bureau of Standards. It was found to emit 2.47 watts  $\text{cm}^{-2} \mu^{-1} \text{ster}^{-1}$  at  $2.2 \mu$ . The relative sensitivity of the optical system and detector at  $4.5$  and  $2.2 \mu$  was then determined by viewing a blackbody source of known temperature at the two wavelengths.

With the foregoing calibration factors at hand, the absolute spectral emission,  $I_g$ , of the hot gas at  $4.5 \mu$  is readily determined from the following formula:

$$I_g = (V_g/V_s) (I/R) (I/t_w) I_s \quad (3)$$

where

$V_g$  = amplitude of emission signal, volts

$V_s$  = amplitude of signal from internal standard source, volts

$R$  = sensitivity of the system at  $4.5 \mu$  relative to that at  $2.2 \mu$

$t_w$  = transmittance of shock-tube window at  $4.5 \mu$ .

$I_s$  = intensity of internal standard at  $2.2\mu$ .

This formula is valid provided the amplification and the slit width are the same when both  $V_g$  and  $V_s$  are recorded. If they are not the same, the appropriate correction terms must be applied.

#### Shock Tube

The shock tube was of rectangular cross section, 37mmx74mm. Two circular sapphire windows, 28mm in diameter, were flush-mounted opposite one another across the longer dimension. The midpoint of the windows was 3.94 meters from the polyester plastic diaphragm which separated this driven section of the shock tube from the driver section. The midpoint of the windows was 179 mm from the downstream end wall of the driven section. This distance to the end wall could be reduced to 27mm or to 78mm by means of close-fitting plugs. The driver gas was helium. The diaphragms were pressure-burst.

#### Timing, Pressure, and Recording Instrumentation

Four thin-film resistance gauges were mounted upstream of the windows and one at the same axial position as the centerline of the windows.



1 These gauges marked the time of incident (and in some cases, reflected)  
2 shock arrival at the five positions, relative to the first, or trigger,  
3 position. The signals were displayed on one beam of a dual beam  
4 oscilloscope. The other beam displayed the output of a quartz pressure  
5 transducer. This transducer was also located at a position corresponding  
6 to the centerline of the windows. A second dual beam oscilloscope was  
7 triggered to display absorption and emission levels from the gas as  
8 measured by the IMRA apparatus. Timing pulses from a crystal-controlled  
9 secondary frequency standard were recorded on all four oscilloscope beams  
10 for each run. A calibration signal for the emission level interrupted  
11 about 1100 times per second for identification and a calibration signal  
12 for the pressure were also recorded each time. Figure 3 shows the oscillograph  
13 records of infrared absorption and emission for a single experiment. The  
14 important features of this typical record are: (1) the large changes of  
15 intensity of transmitted and emitted light upon passage of the shock waves,  
16 (2) the relatively noise-free signals; and (3) the quick recovery of the  
17 tuned amplifier in the absorption channel from the ringing induced by

step-changes, permitting meaningful readings to be made about 50  $\mu$  sec after passage of the shock.

It will be noted in figure 3 that the gas behind the reflected shock was practically black in this particular run. That is, it absorbed all of the radiation from the glower source. In many runs of this sort, the portion of the absorption trace after the reflected shock was simultaneously displayed on another oscilloscope at much higher gain, so that the absorptivity could be accurately determined.

#### Test Gas

A commercially prepared argon-carbon dioxide mixture was used without further treatment. It analyzed 9.9% carbon dioxide by volume, the balance, argon. A few tests were made with this gas diluted to 6.7% carbon dioxide in argon and with a commercially prepared argon-carbon dioxide mixture which analyzed at 1.1% carbon dioxide, the balance, argon.

## RESULTS AND DISCUSSION

The results of determinations of gas temperatures behind incident shocks are presented in *fig. 4*, where they are compared with temperatures calculated by simple shock theory from measured shock velocities. The IMRA temperatures were actually measured at several 10- $\mu$ sec intervals for each experiment, starting at about 50  $\mu$ sec laboratory time when the signals first became readable. Each point in figure 4 was obtained by extrapolating such data back to time zero, the instant when the shock passed the center of the windows. This was done to eliminate effects of attenuation on the temperature.

The agreement is good, and as expected, does not seem to be affected by the CO<sub>2</sub> concentration over the range studied.

Despite this general agreement between measured and calculated incident temperatures, there is nevertheless a good deal of scatter evident in figure 4. Part of this scatter is traceable to contamination of the shock-tube windows, but most of it is due to a drifting type of instability of the infrared detector. From run to run, this instability produced

uncertainties as large as 10 percent in the first term of equation (3);  
 the result is an uncertainty of only about 30° at temperatures near 1000° K,  
 but this grows to nearly 300° at temperatures near 4000° K.

Inasmuch as the main purpose of the work was to measure reflected-shock temperatures at levels above 2000° K, it was desirable to reduce the expected scatter in the results as much as possible. This was done by using the incident shock wave as an internal standard for each run.

The temperature calculated from the measured shock velocity at the window position, and the measured emissivity of the gas behind the incident wave, were both assumed to be correct. The value of spectral emission  $I_g$  required to satisfy equations (1) and (2) was then calculated. This value, and the measured voltages  $V_g$  (incident shock) and  $V_s$ , were inserted in equation (3) and used to calculate a lumped instrument factor,  $(1/R)(1/t_w)I_s$ .

In each run, then, this individually-determined factor was used to convert measured voltages into a series of reflected-shock temperatures, starting at about 50  $\mu$ sec behind the shock and determined at approximately 10- $\mu$ sec intervals. These data were extrapolated to time zero, the instant

1 the reflected shock passed the center of the windows. The resulting  
2 temperatures are plotted as ordinates in figure 5; as abscissas, we have  
3 used the reflected temperatures calculated from the velocity of the incident  
4 shock as it passed the windows, using Markstein's method (ref. 8).

5 This means of obtaining calculated reflected-shock temperatures for  
6 comparison with measured values is clearly rather arbitrary. Its most  
7 obvious shortcoming is that it does not allow for the attenuation of the  
8 incident wave. However, it is important to see how well the temperatures  
9 calculated in this simple way agree with the measured values. Figure 5  
10 shows that they agree surprisingly well. The points obtained with the  
11 end wall at its most remote position, 179mm from the windows, tend to be  
12 high, and those obtained with the end wall 78mm away tend to be low.  
13 This behavior is not inconsistent with that noted in reference 9, which  
14 reported that the reflected-shock pressure behaved as if the shock  
15 decelerated and then accelerated as it receded from the end wall. But  
16 in a grosser sense, the agreement between measured and simply-calculated  
17 temperatures is very gratifying. Of the 27 measurements shown in figure 5,

1 14 are within  $100^\circ$  of the line, and only 4 miss it by more than  $200^\circ$  K.

2 We do however, believe that deviations larger than  $100^\circ$  are real, and

3 that they reflect actual departures of the shocks from ideal one-dimensional

4 behavior.

5 An example of the detail which it is possible to obtain by the IMRA  
6 method, is given in figure 6, where the temperature history of a shock  
7 is followed at 10 to 20  $\mu\text{sec}$  intervals for 700  $\mu\text{sec}$  after its passage.

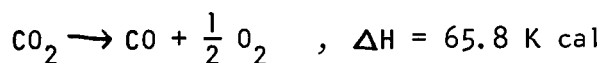
8 The rise in temperature behind the incident shock is accounted for  
9 by attenuation effects. This shock was determined to be attenuating in  
10 velocity at the rate of  $1.5 \times 10^{-4} \text{ mm}/\mu\text{s}/\text{mm} \left( = \frac{dU}{dg} \right)$ , and therefore, for  
11  $10^{-6} \text{ sec}$ ,  $\frac{dU}{U} = 1.5 \times 10^{-4}$ . Strong shock theory predicts  $\frac{dT}{T} = \frac{dP}{P} = 2 \frac{dU}{U}$ .  
12 (Calculations at temperatures of the order of  $1300^\circ \text{ K}$ , show  $\frac{dT}{T} \approx \frac{7}{4} \frac{dU}{U}$  and  
13  $\frac{dP}{P} \approx 2 \frac{dU}{U}$ ). Pressure measurements gave  $dP/P = 3.8 \times 10^{-4}$  behind the  
14 incident shock, somewhat higher than would have been indicated by attenuation.  
15 The IMRA results in figure 6 show  $dT/T = 3.0 \times 10^{-4}$ , in good accordance with  
16 the attenuation prediction.

17 Other observers (ref. 2) have noted a rise in pressure behind reflected

shocks. This pressure rise, converted into an isentropic temperature change by the equation  $T = \left(\frac{P}{P_o}\right)^{\frac{\gamma-1}{\gamma}} T_o$ , corresponds very well with the infrared pyrometer results of *figure 6*.

A second example of detailed analysis is presented in *figure 7*.

Here the temperature following the passage of the reflected shock tends to rise, due to isentropic compression, and tends to decrease due to dissociation according to the equation



(The rate of oxygen atom recombination is sufficiently high so that the concentration of  $\text{O}_2$  is much greater than that of  $\text{O}$  at this temperature).

Using: (1)  $2.9 \times 10^7 \text{ cc moles}^{-1} \text{ sec}^{-1} \text{ } ^\circ\text{K}^{-1}$  for the dissociation rate of  $\text{CO}_2$  at  $3220^\circ\text{K}$  (ref. 10) and for the subsequent temperatures after the reflected shock wave passage, (2.) the isentropic temperature corrections from the measured pressures, and (3.) negligible back reaction of the  $\text{CO}$  and  $\text{O}$  to form  $\text{CO}_2$ , theoretical temperature calculations were made. As with the simpler case of *figure 6*, the agreement of theory and results is gratifying. In this case, *figure 7*, the attenuation comparisons behind

1 the incident shock are  $\frac{dU}{U} = 2.6 \times 10^{-4}$ ,  $\frac{dP}{P} = 4.3 \times 10^{-4}$ , and  $\frac{dT}{T} = 3.4 \times 10^{-4}$ .

## 2 CONCLUSIONS

3 1. Infrared pyrometry of a carbon dioxide-argon gas mixture yielded  
4 temperatures in agreement with those calculated from the incident shock  
5 speed by common shock theory, from 1100 to 3600° K.

6 2. A comparison of reflected shock temperatures measured 27, 78, and  
7 179mm after reflection with temperatures calculated from one-dimensional  
8 shock theory shows latter are *generally good but sporadically may be in error*  
*by large amounts.*

9 3. Attenuation of the speed of an incident shock wave was accompanied  
10 by changes in the gas pressure and temperature in the period following  
11 the passage of the shock. The relationships between these changes ~~were~~ in  
12 general agreement with strong shock theory.

13 4. The change in gas temperature with time after a reflected shock  
14 was adequately calculated from the dissociation rate of carbon dioxide  
15 and the pressure history of the gas mixture.

16 5. These data were preliminary in nature. It is expected that  
17 refinements in apparatus and technique will yield much improved data.

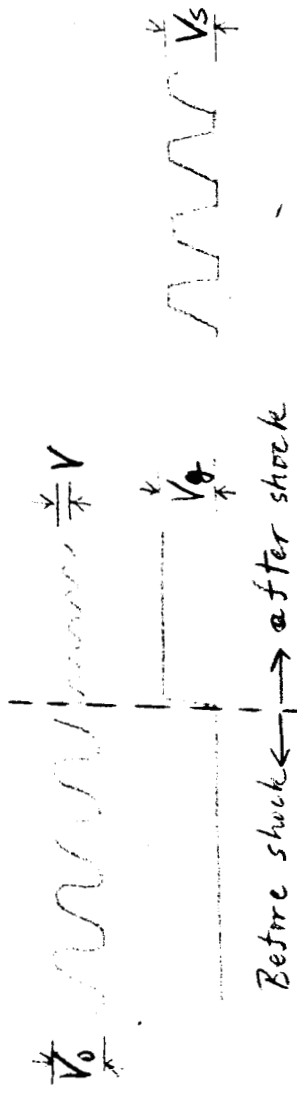


## 1 REFERENCES

- 2 1. Mark, Herman: The Interaction of a Reflected Shock Wave with the  
3 Boundary Layer in a Shock Tube NACA TM 1418, 1958
- 4 2. *Rudinger, George: Effect of Boundary Layer Growth in a Shock Tube*  
5 *on Shock Reflection from a Closed End. Phys. Fluids. Vol. 4, No. 12,*  
6 *Dec. 1961, pp 1463-1473.*
- 7 3. Napier, D. H., Nettleton, M., Simonson, J. R., and Thackeray, D.P.C.:  
8 Temperature Measurement in a Chemical Shock Tube by Sodium-Line  
9 Reversal and  $C_2$  Reversal Methods. AIAA, Journ., Vol. 2, No. 6,  
10 June 1964, pp 1136-1138.
- 11 4. Hurle, I.R., Russo, A.L., and Hall, J. Gordon: Jour. Chem. Phys.  
12 Vol. 40, No. 8, April 15, 1964, pp 2076-2089
- 13 5. Johnson, C.D. and Britton, Doyle: Shock Waves in Chemical Kinetics:  
14 The Use of Reflected Shock Waves. Jour. Chem. Phys. Vol. 38, No. 7,  
15 April 1, 1963, pp 1455-1462
- 16 6. Tourin, Richard H.: Monochromatic Radiation Pyrometry of Hot Gases,  
17 Plasmas, and Detonations. Temperature - Its Measurement and Control  
in Science and Industry. Vol. 3, Part 2, ed., Reinhold Publishing Corp.,  
1962.

- 1 7. Tourin, R. H., Hecht, M.L., and Dolin, S.A.: Measurement of Gas  
2 Temperatures in Thermal Pulses by Monochromatic Radiation Pyrometry  
3 Part 2 of Final Report under Contract 33(616)-6713 with Aero. Res.  
4 Lab., Office of Aerospace Research, U.S. Air Force, Wright-Patterson  
5 Air Force Base, Ohio
- 6 8. Markstein, George H.: Graphical Computation of Shock and Detonation  
7 Waves in Real Gases. ARS Journ., Vol. 29, No. 8, Aug. 1959,  
8 pp. 588-590.
- 9 9. Brabbs, T.A., Zlatarich, S.A., and Belles, F.E.: Limitations of the  
10 Reflected-Shock Technique for Studying Fast Chemical Reactions.  
11 Journ. Chem. Phys., Vol. 33, No. 1, July, 1960, pp 307-308.
- 12 10. Brabbs, T.A., Belles, F.E., and Zlatarich, S.A.: Shock-Tube Study  
13 of Carbon Dioxide Dissociation Rate. Jour. Chem. Phys., Vol. 38,  
14 No. 8, April 15, 1963, pp 1939-1944.
- 15  
16  
17

FIG 1 BASIS OF IMPA  
TEMPERATURE MEASUREMENT



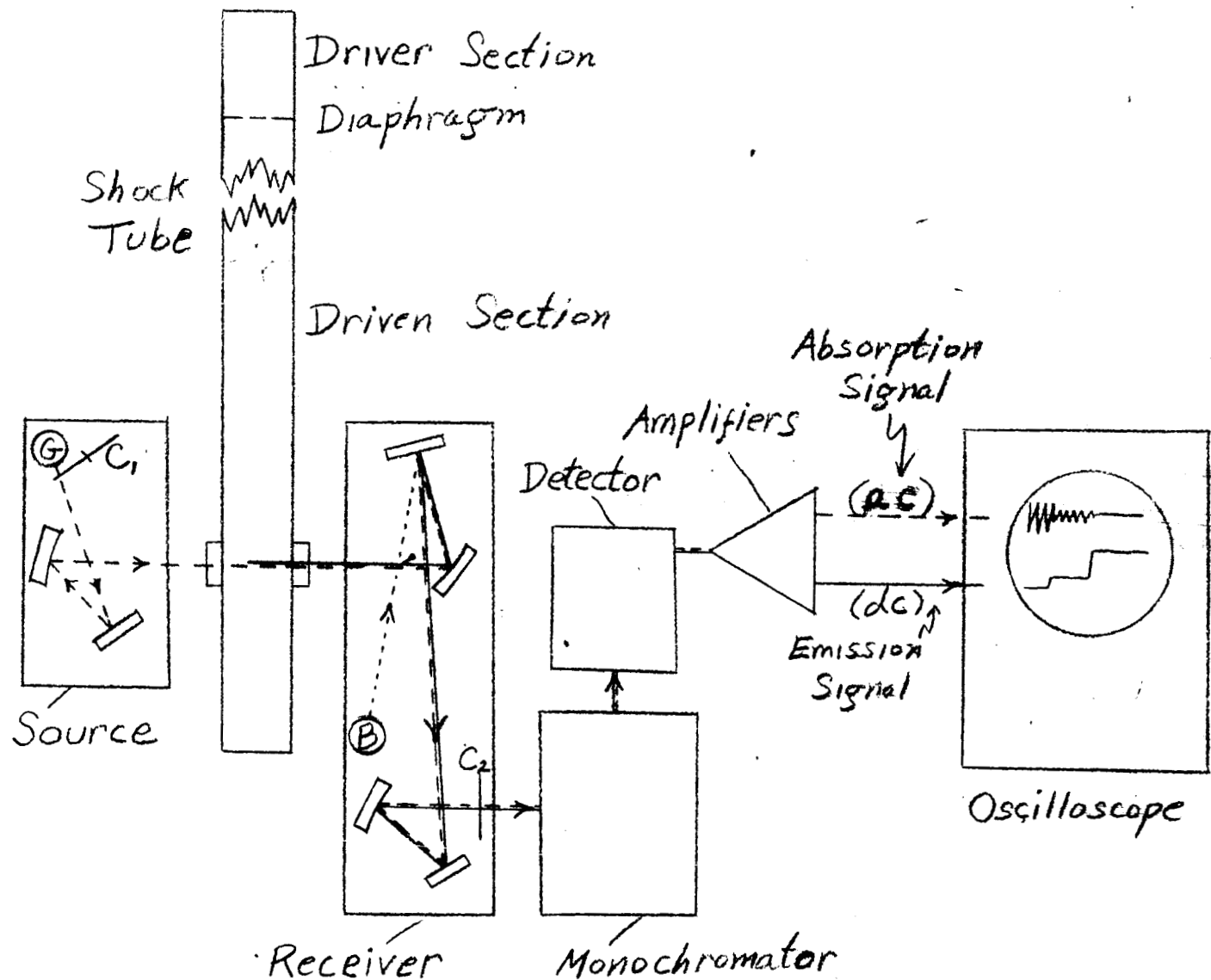
1. Emissivity,  $e = \text{Absorptivity} = 1 - (V/V_0)$

2. Kirchhoff's Radiation Law:

$$\frac{\text{Spectral Emission, } I_\lambda}{\text{Spectral Emissivity, } e} = \frac{\text{Spectral Emission of Blackbody at same Temperature, } I_b}{e}$$

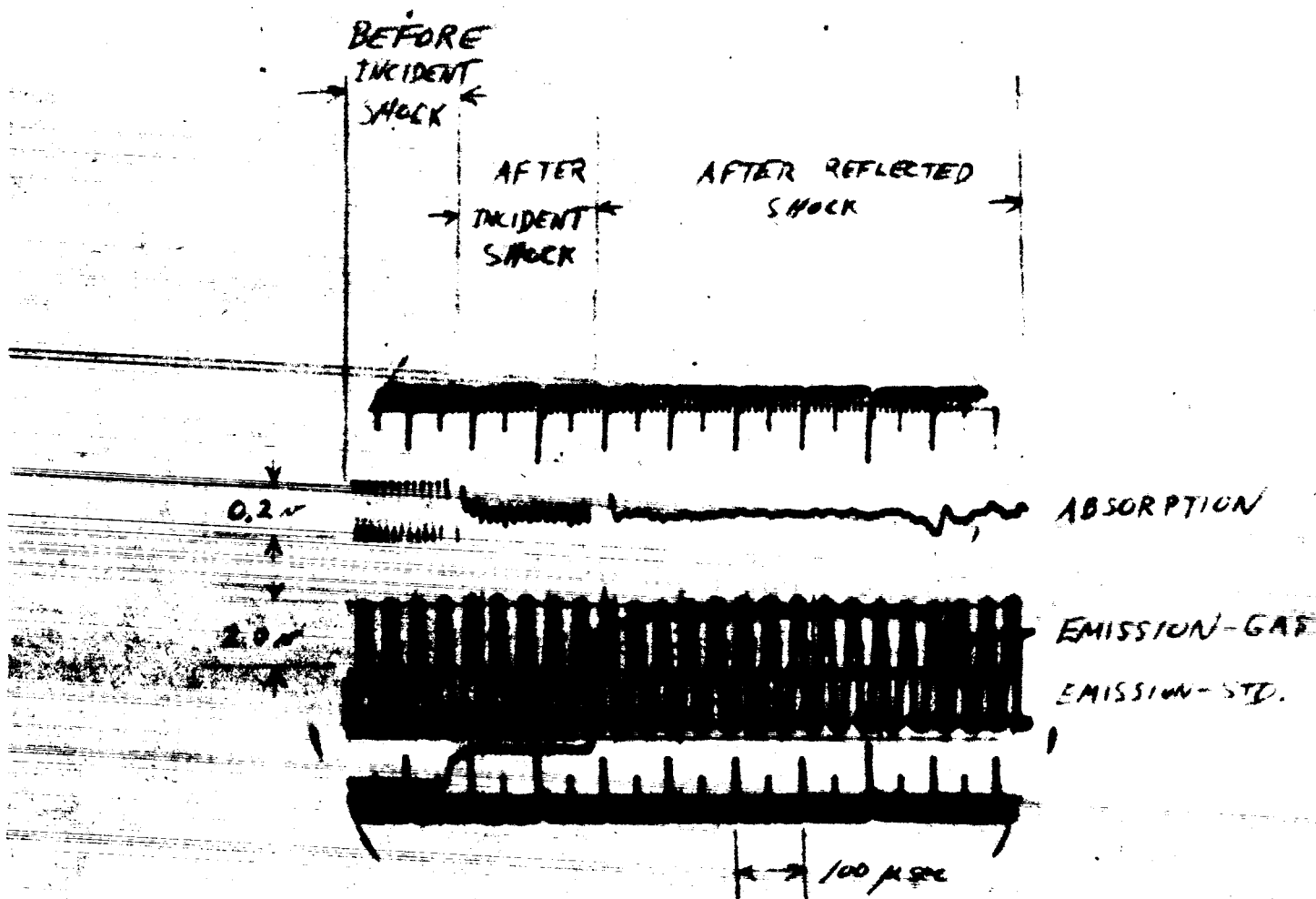
3. Planck's Law:  $I_b = c_1 \lambda^{-5} / (e^{c_2/\lambda T} - 1)$

Figure 2. — Schematic Diagram of a Monochromatic Radiation Pyrometer.



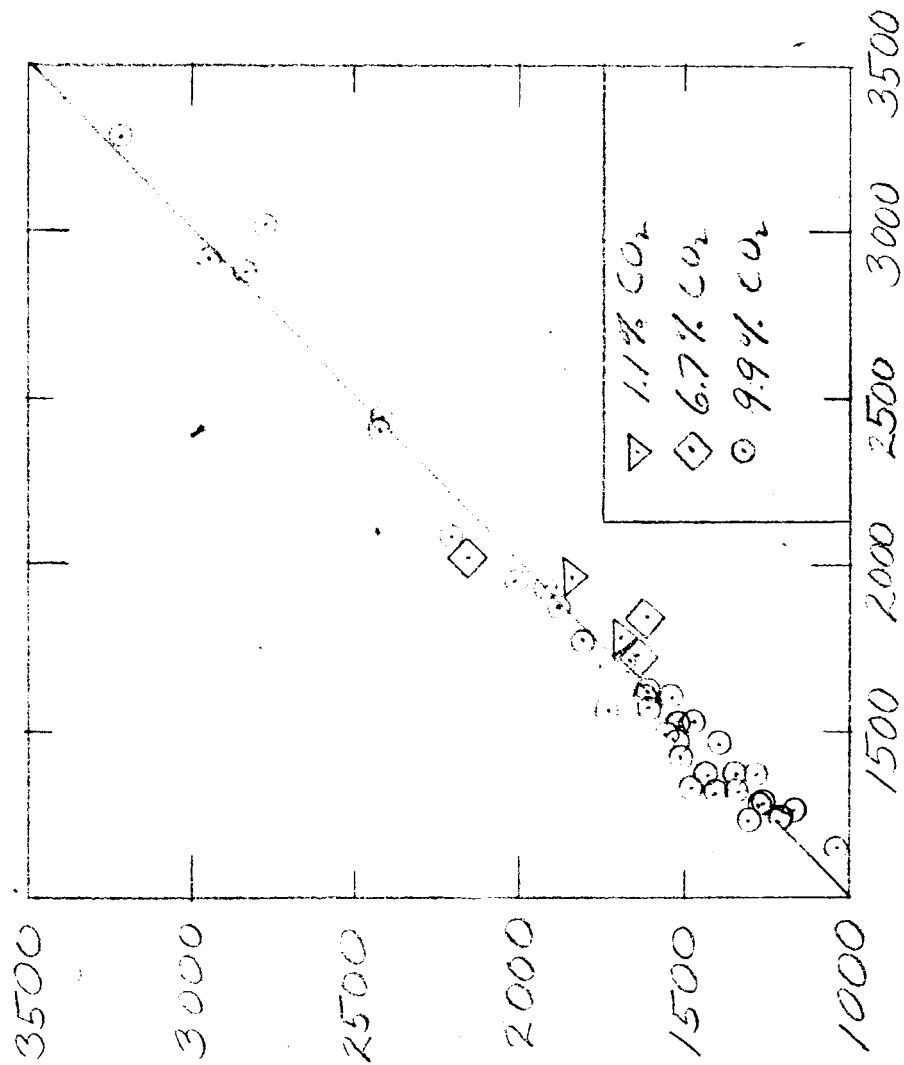
- G Glower
- B Internal Standard
- C<sub>1</sub> 80 kcps Chopper
- C<sub>2</sub> 1.1 kcps Chopper

FIG. 3 Typical Oscillogram



7-29-64-1610

FIG. 4 COMPARISON OF IMRA-DERIVED AND SHOCK VELOCITY-DEIVED TEMPERATURES BEHIND INCIDENT SHOCKS IN  $\text{CO}_2$ -ARGON



(11-5, 197)

FIG. 5 COMPARISON OF IMRA-DEIVED AND  
 TEMPERATURES  
 BEHIND REFLECTED - MUCKS 14.00% ARSON.

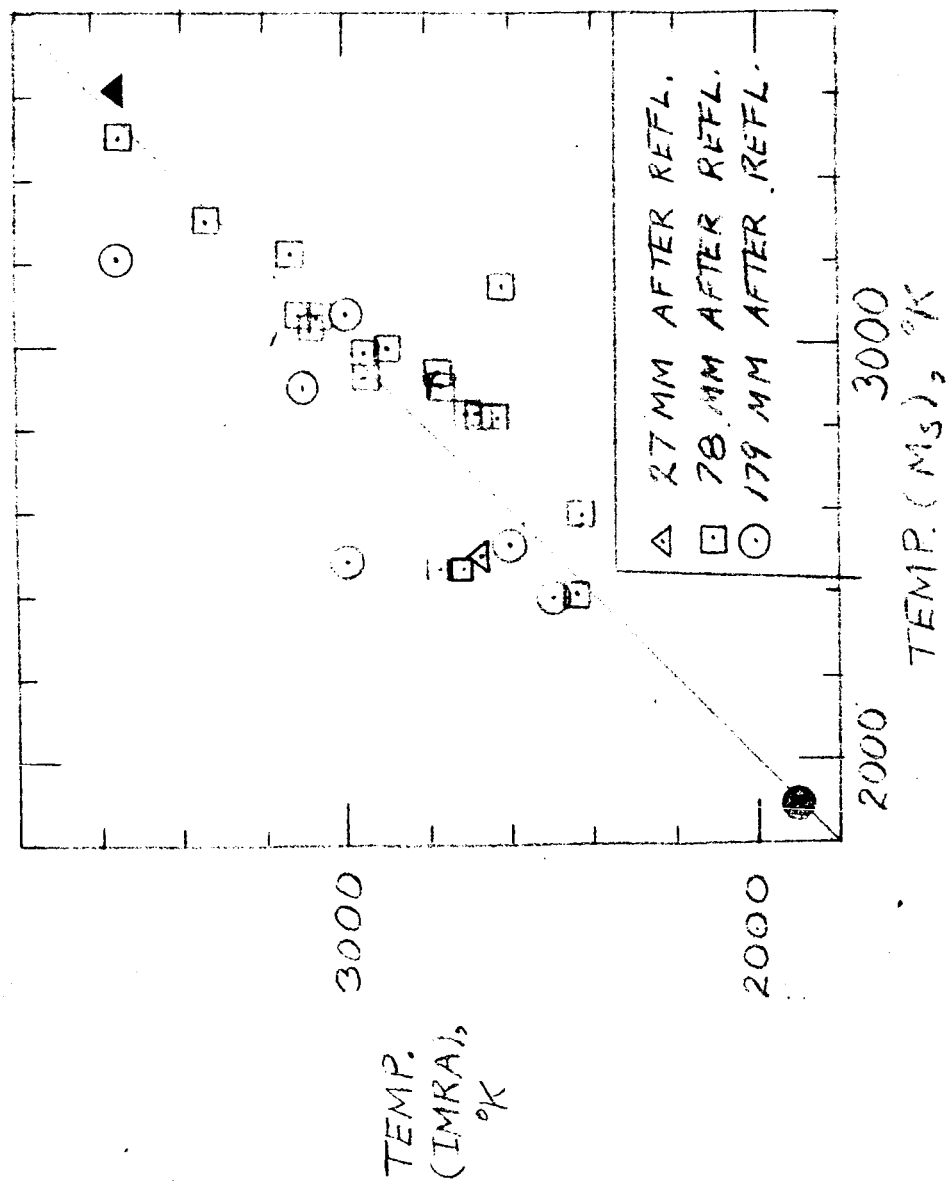


FIG. 6 EXPERIMENTAL AND CALCULATED TEMPERATURES BEHIND SHOCK WAVES IN  $\text{CO}_2$  - ARGON.  $P_1 = 81.2 \text{ torr}$ ,  $M_s = 3.64$

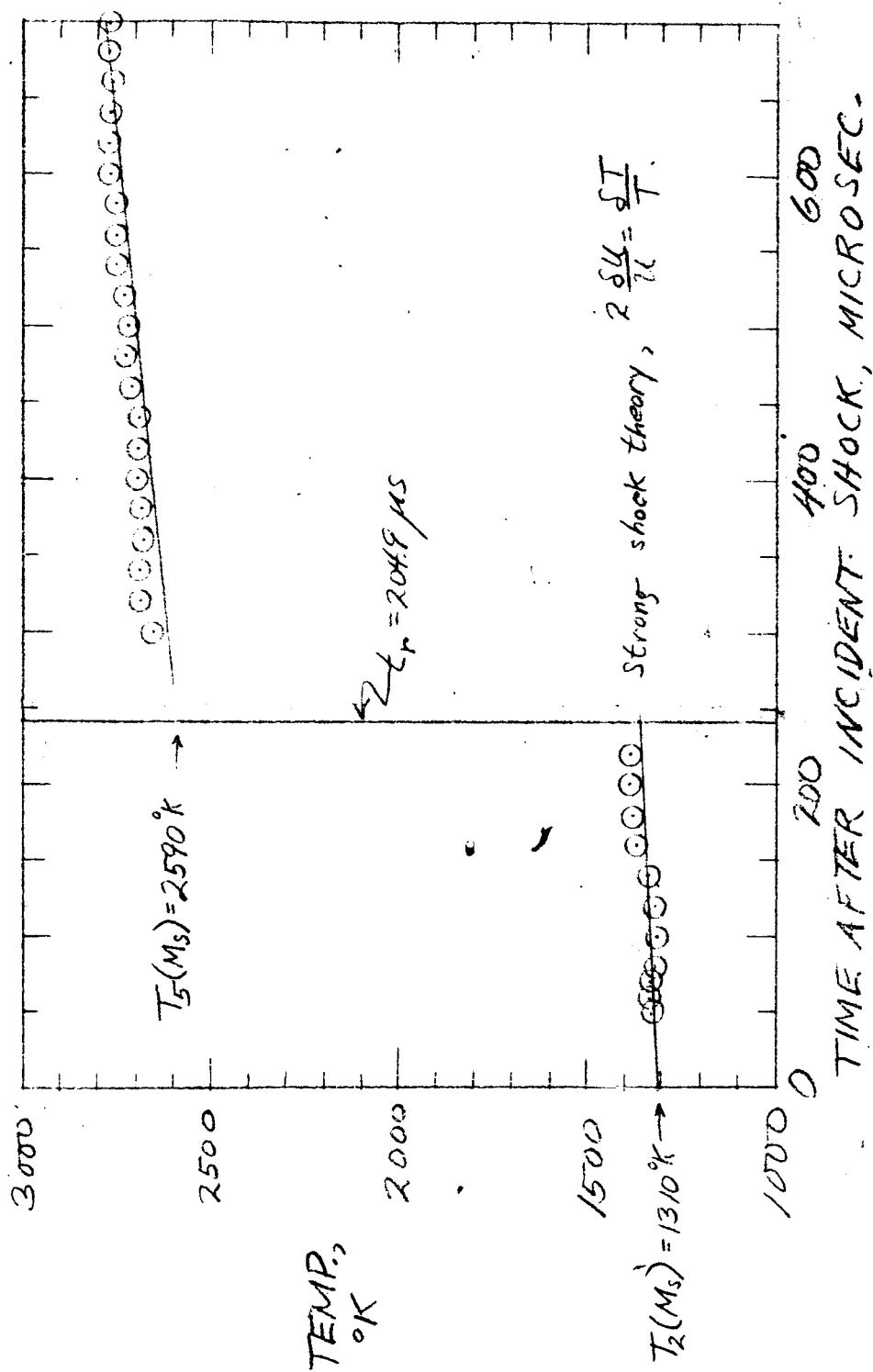




FIG. 7. EXPERIMENTAL AND CALCULATED TEMPERATURES BEHIND SHOCK WAVES IN  $\text{CO}_2$  - ARGON.  $P_i = 51.0 \text{ Torr}$ ,  $M_s = 4.09$ .

